

MPACT Fast Neutron Multiplicity System Prototype Development

D. L. Chichester
S. J. Thompson
S. A. Pozzi
J. L. Dolan
M. T. Kinlaw
M. Flaska
J. T. Johnson

September 2013



**INL is a U.S. Department of Energy National Laboratory
operated by Battelle Energy Alliance**

DISCLAIMER

This information was prepared as an account of work sponsored by an agency of the U.S. Government. Neither the U.S. Government nor any agency thereof, nor any of their employees, makes any warranty, expressed or implied, or assumes any legal liability or responsibility for the accuracy, completeness, or usefulness, of any information, apparatus, product, or process disclosed, or represents that its use would not infringe privately owned rights. References herein to any specific commercial product, process, or service by trade name, trade mark, manufacturer, or otherwise, does not necessarily constitute or imply its endorsement, recommendation, or favoring by the U.S. Government or any agency thereof. The views and opinions of authors expressed herein do not necessarily state or reflect those of the U.S. Government or any agency thereof.

MPACT Fast Neutron Multiplicity System Prototype Development

**D. L. Chichester¹, S. J. Thompson¹, S. A. Pozzi², J. L. Dolan², M. T. Kinlaw¹,
M. Flaska², and J. T. Johnson¹**

¹ Idaho National Laboratory

² Department of Nuclear Engineering & Radiological Sciences,
University of Michigan

September 2013

**Idaho National Laboratory
Idaho Falls, Idaho 83415**

<http://www.inl.gov>

**Prepared for the
U.S. Department of Energy
Office of Nuclear Energy
Under DOE Idaho Operations Office
Contract DE-AC07-05ID14517**

ACKNOWLEDGEMENTS

The authors would like to kindly acknowledge the support of Dr. Paolo Peerani, his research colleagues Mrs. Alice Tomanin and Mr. Santino Frison, and other staff at the European Commission's PERLA Laboratory at the Joint Research Center in Ispra, Italy. Without his interest in our work, his desire to collaborate with our research team, and his support in hosting us at his laboratory, work that took place at JRC-Ispra in 2011 through 2013 would not have been possible.

We would like to thank Dr. Paul Hausladen for his suggestions and thoughtful commentary on this work.

The work in this report was sponsored by the U.S. Department of Energy's Fuel Cycle Research and Development program and its Materials Protection, Accounting, and Control Technologies (MPACT) program. The authors would also like to acknowledge and thank Dr. Mike Miller, technical director for the MPACT program for his support and enthusiasm of this research project.

We would also like to acknowledge and thank the Nuclear Forensics Graduate Fellowship Program, which is sponsored by the U.S. Department of Homeland Security, Domestic Nuclear Detection Office and the U.S. Department of Defense, Defense Threat Reduction Agency, for supporting some of the activities of this project.

Congratulations to Dr. Dolan!

EXECUTIVE SUMMARY

This document serves as both an FY2103 End-of-Year and End-of-Project report on efforts that resulted in the design of a prototype fast neutron multiplicity counter leveraged upon the findings of previous project efforts. The prototype design includes 32 liquid scintillator detectors with cubic volumes 7.62 cm in dimension configured into 4 stacked rings of 8 detectors. Detector signal collection for the system is handled with a pair of Struck Innovative Systeme 16-channel digitizers controlled by in-house developed software with built-in multiplicity analysis algorithms. Initial testing and familiarization of the currently obtained prototype components is underway, however full prototype construction is required for further optimization.

Monte Carlo models of the prototype system were performed to estimate die-away and efficiency values. Analysis of these models resulted in the development of a software package capable of determining the effects of nearest-neighbor rejection methods for elimination of detector cross talk. A parameter study was performed using previously developed analytical methods for the estimation of assay mass variance for use as a figure-of-merit for system performance. [1, 2] A software package was developed to automate these calculations and ensure accuracy. The results of the parameter study show that the prototype fast neutron multiplicity counter design is very nearly optimized under the restraints of the parameter space.

Also of note, Jennifer L. Dolan, a graduate student that has been a part of the project from its onset, successfully defended her doctoral dissertation in May of 2013.

CONTENTS

ACKNOWLEDGEMENTS	ii
EXECUTIVE SUMMARY	iv
1 INTRODUCTION	1
1.1 Advanced Fuel Cycle Materials and MPACT	2
1.2 Relevance for International Safeguards	3
2 MULTIPLICITY COUNTING	3
2.1 Traditional Counting with Gates	4
2.2 Multiplicity Analysis	5
2.3 Motivation for Fast-Neutron Counting	7
2.3.1 Fast-Neutron Multiplicity Objectives	7
2.3.2 Performance Improvements	7
3 UNIVERSITY EFFORTS	10
4 FAST NEUTRON MULTIPLICITY COUNTER PROTOTYPE DESIGN	11
4.1 Prototype Performance Comparison	14
4.2 Analytical Parameter Study	18
4.3 Current Prototype Status	21
5 SUMMARY	24
6 REFERENCES	24

FIGURES

Figure 1. Calculated RSD (%) versus sample mass for representative detection systems. Left: slow die-away system with $\tau = 50 \mu\text{s}$, $G = 1.257\tau$, $P_d = 1.5 \mu\text{s}$, and $\varepsilon = 0.35$. Right: fast die-away system (solid lines) with $\tau = 10 \text{ ns}$, $G = 1.257\tau$, $P_d = 1.5 \text{ ns}$, and $\varepsilon = 0.35$. Calculations for the longer die-away system (broken lines) are included for comparisons.....	9
Figure 2. Calculated RSD (%) versus detector die-away times for representative detection systems. Left: short predelay with $G = 1.257\tau$, $P_d = 1.5 \text{ ns}$, and $\varepsilon = 0.35$. Right: typical thermal neutron detection system predelay with $G = 1.257\tau$, $P_d = 1.5 \mu\text{s}$, and $\varepsilon = 0.35$	10
Figure 3. Linear and quadratic fits to PuO ₂ double coincidence detection rates versus effective ²⁴⁰ Pu mass.....	11
Figure 4. Side and top-down views of the FNMC prototype design from an MCNPX model.....	12
Figure 5. Rossi-Alpha distribution generated from the simulation of a 60 second long measurement of a 1.0 μCi ²⁵² Cf source. The application of nearest-neighbor rejection methods is shown in blue.....	14
Figure 6. Percent mass variance as a function of assay time for several different measurement scenarios. Values for the FNMC are represented with solid lines, while those for the JCC-31 are shown with dashed lines. Values are given for ²⁴⁰ Pu masses of 100 g (top) and 1 kg (bottom).....	16
Figure 7. Assay variance for the prototype FNMC (top) and the HLNCC (bottom) as a function of ²⁴⁰ Pu mass. Values are provided for 60-s (blue), 300-s (red) and 600-s (black) measurement periods. High-multiplication low-alpha and low-multiplication high-alpha rate scenarios are shown by solid and dashed lines respectively.....	17
Figure 8. Assay variance for the prototype FNMC as a function of neutron detection efficiency. Values are provided for 60-s (blue), 300-s (red) and 600-s (black) measurement periods. High-multiplication low-alpha and low-multiplication high-alpha rate scenarios are shown by solid and dashed lines respectively.....	19
Figure 9. Assay variance for the prototype FNMC as a function of coincidence window width. Values are provided for 60-s (blue), 300-s (red) and 600-s (black) measurement periods. High-multiplication low-alpha and low-multiplication high-alpha rate scenarios are shown by solid and dashed lines respectively.....	20
Figure 10. Assay variance for the prototype FNMC as a function of detection system die-away. Values are provided for 60-s (blue), 300-s (red) and 600-s (black) measurement periods. High-multiplication low-alpha and low-multiplication high-alpha rate scenarios are shown by solid and dashed lines respectively.....	21
Figure 11. Photograph of the Struck model SIS3316 digitizer.....	22
Figure 12. A sample setup from the initial testing of the Struck SIS3316 digitizer.....	22
Figure 13. An example of a neutron time-of-flight measurement using the Struck SIS3316 pulse shape discrimination methods. A single liquid scintillator placed 110 cm from the time tagged ²⁵² Cf source was used to collect the data. Colored regions represent similar pulse shape analysis values for use in neutron/photon	

discrimination. Pulses with pulse heights below 650 keVee were discarded from this data set...... 23

TABLES

Table 1. Calculated absolute threshold values for the FNMC prototype for several pulse height detection thresholds. 13

Table 2. System parameter values used for the analytical performance comparison of the prototype fast neutron multiplicity counter and CANBERRA's JCC-31 High Level Neutron Coincidence Counter...... 15

MPACT Fast Neutron Multiplicity System Prototype Development

1 INTRODUCTION

Idaho National Laboratory (INL) has been working to explore new methods for analyzing nuclear materials using fast, time-correlated measurements for several years. [3, 4, 5] This work, supported by the U.S. Department of Energy's Fuel Cycle Research and Development program and its Materials Protection, Accounting, and Control Technologies (MPACT) program, has been a collaborative effort including staff at INL as well as staff and students in the Department of Nuclear Engineering & Radiological Sciences at the University of Michigan (UM). These activities have included simulation and modeling using the MCNPX-PoliMi Monte Carlo simulation tool and experiments to validate the simulations, development of hands-on experimental methods, and the discovery of pitfalls and challenges in performing these types of measurements that cannot be identified any other way. INL possess a strong background in these areas, notably addressing nuclear security and safeguards challenges, heavily weighted towards real world experiments and system-level development and demonstration efforts, and the use of electronic neutron generators in active neutron interrogation. The University of Michigan team is a recognized world leader in the study and development of the MCNPX-PoliMi computer code for modeling time-correlated measurements, as well as in the use of liquid scintillator-based detector systems for studying and characterizing special nuclear materials and their time-correlated signatures.

This report documents work performed by INL and UM in fiscal year (FY) 2013 to develop a prototype system that uses fast-neutron multiplicity counting for assaying plutonium for materials protection, accountancy, and control purposes. This project seeks to develop a new type of neutron-measurement-based plutonium assay instrument suited for assaying advanced fuel cycle materials. Some current-concept advanced fuels contain high concentrations of plutonium; some of these concept fuels also contain other fissionable actinides besides plutonium. Because of these attributes the neutron emission rates of these new fuels may be much higher, and more difficult to interpret, than measurements made of plutonium-only materials. The most commonly used approach for assaying plutonium is the use of thermal-neutron coincidence and multiplicity counters. However, these instruments can have difficulty when analyzing high-rate neutron sources. Also, there is a strong desire to develop new, alternative plutonium-assay systems that do not rely on the use of helium-3 detectors (as are most often used in thermal neutron systems) due to recent shortages of this material for safeguards applications.

A promising approach in this area is to perform measurements at much faster (nanosecond) time scales versus the longer (microsecond) time scales of thermal neutron systems. Fast-neutron measurements dramatically reduce the negative impacts of random coincidences in correlated-neutron assays that can occur with high count-rate samples. They also allow for in-depth analysis of multiplication phenomena in sample items in comparison with thermal analysis systems. Lastly, faster assay systems have the potential to reduce the burden on facility operators by reducing measurement times and improving the precision of assay measurements. The long-term goals of this project are to design and build a fast neutron multiplicity analysis system for assaying advanced fuel cycle materials and then to test and evaluate this instrument

using these materials. This project supports Objective 4 from the Nuclear Energy Research and Development Roadmap to “minimize the risks of nuclear proliferation and terrorism” and more specifically the Advanced Instrumentation sub-item in the Safeguards and Physical Security Technologies and Systems area "Development of advanced passive detectors such as neutron multiplicity counting." [6]

1.1 Advanced Fuel Cycle Materials and MPACT

As described in previous End-of-Year Reports, advanced nuclear fuels are currently under development within the Department of Energy's Fuel Cycle Research and Development program as part of a long-term research effort focused at understanding the behavior of mixed-oxide (MOX) fuels containing minor actinides and long-lived fission products. [3, 4] The aim of this work is to understand how these materials impact the long-term performance of nuclear fuel in order to be able to design and manufacture advanced fuels for use in next-generation reactors. Reusing, or recycling, the higher actinides and long-lived fission products in advanced nuclear fuels ultimately leads to the transmutation of these materials into shorter-lived waste products which may be more easily and more safely disposed of. There are several potential benefits of reusing nuclear fuel including the reclamation of additional energy content from once-through used fuels, the reduction or removal of longer-lived waste products from spent fuel, and the lessening of the storage demands eventually placed on facilities for the long-term storage or disposal of spent fuels. In parallel with the fuel development projects research and development is also underway to develop advanced fuel reprocessing approaches to produce these fuels and to develop advanced reactors to utilize them. However, in addition to these core engineering research and development projects the ultimate viability of these new technology developments will be critically linked to advances in nuclear safeguards and material protection, accounting, and control technologies (MPACT).

Traditional nuclear safeguard measurement techniques used to monitor uranium oxide fuels are not well-suited for analyzing advanced MOX fuels. Gross gamma-ray counting is complicated by the presence of the additional radioactive materials in the fuel while high-resolution gamma-ray spectroscopy can be difficult to perform due to the presence of multiple interferences associated with the presence of the minor actinides. Similarly, the powerful passive and active neutron-based nondestructive assay techniques used with current-generation fresh and irradiated commercial nuclear fuel are complicated by the presence of multiple higher actinides, some of which have spontaneous fission and induced fission signatures comparable to plutonium. From 2009 through 2012 it has been the goal of the INL-UM collaboration to explore techniques for fast-neutron and photon-correlation measurements, both passively and with active interrogation. The aim of these efforts has been to improve the fundamental understanding of nuclear materials and the physics of detection methods through coupled theory, simulation, and experiment, as necessary to develop next-generation materials management and MPACT technology. More broadly speaking, these efforts have been part of the larger MPACT research portfolio seeking to enhance overall nuclear fuel cycle proliferation resistance via improved technologies for used fuel management.

Important aspects of long-term, science-based, engineering-driven research and development (R&D) include small-scale experiments, theory development, and advanced modeling and simulation with validation experiments. This project embraces this paradigm for the "science-based" R&D approach for improving domestic MPACT approaches for security and safeguards.

1.2 Relevance for International Safeguards

Nuclear safeguards are defined as the effort to prevent diversion of fissile material. In 1970, the Treaty on the Nonproliferation of Nuclear Weapons (NPT) was entered into force with the objective to prevent the spread of nuclear weapons and their technology, while encouraging the peaceful use of nuclear technology. [7] Through the treaty a safeguards system was established. Nuclear safeguards endeavors are the responsibility of the International Atomic Energy Agency (IAEA) and are supported by diplomatic and economic means.

Given the increase in nuclear facilities across the world and innovation in the nuclear fuel cycle, new technology is needed to continue special nuclear material (SNM) accounting, control, and safeguards efforts. Specifically, the planned increase in fuel reprocessing warrants innovation in novel safeguards techniques to minimize the associated nonproliferation risks. The national energy policy has recommended research efforts in the development of reprocessing and fuel treatment technologies that are more proliferation-resistant. Additionally, safeguards designed directly into a new facility will be essential to international safeguards success.

2 MULTIPLICITY COUNTING

Nuclear safeguards rely on technology used during nuclear facility inspections to detect any diversion of fissile material. The most standard form of safeguards confirms the presence and type of materials from a facility's declarations. The technologies used to verify the material declarations include both destructive and nondestructive assay. Nondestructive assay is a preferred method of investigation and can include technologies based on neutron, photon, or calorimetric measurements. All of these concepts have their pros and cons, but neutron measurements remain to be a leading method. Neutrons are more penetrating than other forms of radiation and are they are less prevalent in radiation background and naturally occurring radioactive materials. An added benefit of neutron measurements exists due to the emission of multiple neutrons spontaneously from a single reaction, which is unique to fission. Therefore, neutron multiplicity measurements, where the neutron multiplicity distributions are measured, have continued to rise to the top for characterizing fissile materials in nuclear accountancy applications.

Early characterization systems measured only the neutron rate, which was applicable to only a few types of plutonium containing materials, considering there are other neutron emitting reactions present in many plutonium containing materials. Further developments extended systems into neutron coincidence counters, which provided a method to isolate only the measurement of neutrons from fission and has been extensively applied in safeguards. With the measurement of the neutron fission rate and knowledge of the neutron multiplicity distribution, the mass of certain plutonium isotopes can be identified. Neutron coincidence counting has not been as applicable to domestic accountability considering that only two parameters are measured (singles and doubles) and therefore the system's neutron detection efficiency must be known. For impure plutonium samples, the neutron detection efficiency of the system may change and become a variable due to large amounts neutron scatter or moderation within the sample. To solve this problem, assumptions must be made regarding the amount of (alpha, n) neutrons or the sample multiplicity. For greater accuracy and the minimization of assumptions, neutron multiplicity systems were developed that provide three measured parameters: singles, doubles,

and triples. With a neutron multiplicity system, the goal is to be able to correctly characterize any nuclear fuel cycle material without any knowledge of the material's matrix. [8]

Currently available multiplicity systems are categorized based on the range of plutonium mass they are designed to quantify. For lower masses of plutonium (0.1 to 500 g of plutonium) low-level inventory sample coincidence counters are available from companies like Canberra. [9] High-level systems measure up to several kilograms of plutonium. Both low and high level systems contain just fewer than twenty ^3He tubes. These systems rely on spontaneous fission from the even numbered isotopes of plutonium. Similar systems, such as active-well coincidence counters, can quantify uranium as well but require a neutron active-interrogation source and more than twice as many ^3He tubes. Other systems are designed to measure specific nuclear fuels such as neutron coincidence collars (PWR, BWR, CANDU assemblies), fast-breeder reactor subassembly counters (single or groups of fast-breeder fuel pins), and plutonium scrap counters (impure plutonium samples or MOX). A fast neutron multiplicity counter described and discussed in this report is applicable for all of these measurement scenarios. [10]

2.1 Traditional Counting with Gates

In traditional ^3He systems, when fission occurs in the measured sample and neutrons are emitted, they are moderated in an optimized polyethylene medium and the neutron population exponentially dies away. Neutrons are removed from the detector system by escaping the system, neutron absorption in nearby neutron absorbing materials (such as hydrogen or plutonium), or ideally neutron capture by ^3He . Typical die-away times for ^3He systems are on the order of tens of micro-seconds but are practically nonexistent for fast neutron counters. For each neutron detected a single pulse is generated that is fed through a system of electronics resulting in a single stream of pulses for all of the detectors present in the system. It is then necessary to separate the correlated neutron events (fission events providing the plutonium signature) from the uncorrelated neutron events (events from other neutron emitting reactions and background events). This is done through optimized time-gating of the time-dependent pulse stream. [8]

A common method for identifying correlated events is through shift-register circuits based on the concept of a Rossi-alpha distribution. [8] The Rossi-alpha distribution is the distribution in time of events that occur after a randomly chosen start event. This distribution will be constant with time if only uncorrelated events are detected and therefore will have features when correlated events are present. The distribution is defined by the constant uncorrelated events plus the exponentially decaying "Real" or correlated events. Time gates are then defined to isolate the "Reals + Accidentals" portion and the "Accidentals" portion of the distribution. The "Reals + Accidentals" gate will be on the order of tens of micro-seconds, and then there will be a long delay (on the order of thousands of micro-seconds) before the "Accidentals" gate is opened for a time more similar to the initial gate. An actual measured distribution will not increase exponentially as you take the limit to zero, due to pulse pile-up and electronic dead-time effects. Therefore, a "pre-delay" time gate is also specified to correct for these limiting effects.

Identification of only the "Reals" leads to the indication of the multiplicity distribution and furthermore the fission rate, which is necessary to determine the plutonium mass. [8] Specialized electronics exist to take the stream of pulses and isolate the time-gates to identify the neutron multiplicity distributions for both the "Reals + Accidentals" and "Accidentals" gates. The result of analyzing and unfolding both sets of data is the singles, doubles, and triples values

needed for eventual mass quantification. [8] A fast neutron multiplicity counter can directly provide these three parameters without the circuitry and unfolding.

2.2 Multiplicity Analysis

One of the primary purposes of utilizing neutron multiplicity counting over traditional neutron coincidence counting lies in the extension of possible parameters that can be determined. With coincidence counting, m_{240eff} , the ^{240}Pu effective mass (i.e., the mass of ^{240}Pu that will produce a coincidence rate equivalent to the sum of all isotopes in the sample with a high propensity to undergo spontaneous fission) is determined according to the following equation:

$$m_{240eff} = 2.52 \cdot m_{238} + m_{240} + 1.68 \cdot m_{242}$$

where m_{238} , m_{240} , and m_{242} are the sample masses of ^{238}Pu , ^{240}Pu , ^{242}Pu respectively. [8] However, in cases where additional parameters are sought, such as the (α,n) reaction rate, additional information is also required. For multiplicity counting, this additional information is gleaned by measuring, in addition to the first and second moments, the third moment of the detected neutron distribution. With these three moments, the sample multiplication, fission rate, and (α,n) reaction rate can each be calculated. The calculations and equations shown below have been derived in numerous reports and publications. [8, 1, 11]

The detected neutron singles rate, S , represents all neutrons detected, regardless of their reaction of origin, including those emitted via spontaneous fission, induced fission, and (α,n) reactions. Empirically, this rate can be calculated as:

$$S = F\varepsilon M\nu_{i,1}(1 + \alpha)$$

where F is the spontaneous fission rate of the sample (~ 479 neutrons per second per gram of ^{240}Pu), ε represents the absolute detection efficiency, M is the sample multiplication (leakage), and α is the alpha fraction. [8, 1, 12] Factorial moments in this report are represented by the character ν with a primary subscript of 's' or 'i' denoting whether it is a moment of the multiplicity distribution of the spontaneous fission of ^{240}Pu or the induced fission of ^{239}Pu respectively. For all calculations described in this report the multiplicity distribution for fission induced by a 2 MeV neutron was used to determine all ν_i factorial moments. [13] The secondary subscript on the factorial moment variable denotes the order of the moment (i.e. $\nu_{s,3}$ represents the third factorial moment of the multiplicity distribution of the spontaneous fission of ^{240}Pu).

The detected neutron doubles rate, D , is dependent on spontaneous fission, induced fission, and (α,n) reactions. However, the spontaneous fission and (α,n) terms depend on the second moments, and the induced fission term relates to induced fissions resulting from the multiplication of spontaneous fission neutrons.

$$D = \frac{F\varepsilon^2 M^2 f}{2} \left[\nu_{s,2} + \left(\frac{M-1}{\nu_{i,1}-1} \right) \nu_{s,1}(1+\alpha)\nu_{i,2} \right]$$

In this equation f is the gate fraction given by the equation:

$$f = e^{-Pd/\tau}(1 - e^{-G/\tau})$$

where G is the counting gate width in time, P_d is the predelay for this gate, and τ is the intrinsic die-away of the detection system.

Many different processes can contribute to the detection of three neutrons within a counting interval. The empirical representation of the triples rate is given by:

$$T = \frac{F\varepsilon^3 M^3 f^2}{6} \left[v_{s,3} + \left(\frac{M-1}{v_{i,1}-1} \right) [3v_{s,2}v_{i,2} + (1+\alpha)v_{s,1}v_{i,3}] + \left(\frac{M-1}{v_{i,1}-1} \right)^2 (1+\alpha)v_{s,1}v_{i,2}^2 \right].$$

In this form, an assumption is made where the detector die-away may be approximated, at a minimum, as a single exponential die-away. Hence, the triples gate fraction f_i is simply the square of the doubles gate fraction. If this approximation does not suffice, a more appropriate expression for the triples gate fraction is provided by Eq. 6-6 in Reference 6.

As stated above, the primary advantage of including the third moment of the detected neutron distribution is an ability to determine from the three measured moments the sample multiplication, fission rate (thus the ^{240}Pu effective mass), and (α, n) reaction rate. The sample multiplication can be derived as the positive real solution to the cubic equation:

$$a_0 + a_1 M + a_2 M^2 + a_3 M^3 = 0$$

where

$$a_0 = -T,$$

$$a_1 = D \left[\frac{v_{s,3}}{v_{s,2}} - \frac{3v_{i,2}}{(v_{i,1}-1)} \right],$$

$$a_2 = S \left[\frac{v_{i,2}v_{s,3}}{(v_{i,1}-1)v_{s,2}} - \frac{v_{i,3}}{(v_{i,1}-1)} \right] + D \left[\frac{3v_{i,2}}{(v_{i,1}-1)} \right],$$

and

$$a_3 = S \left[\frac{v_{i,3}}{(v_{i,1}-1)} - \frac{v_{i,2}v_{s,2}}{(v_{i,1}-1)v_{s,2}} \right]. \quad [12]$$

The multiplication can then be used to calculate the fission rate using

$$F = \frac{D - \frac{SM(M-1)v_{i,2}}{(v_{i,1}-1)}}{\varepsilon M^2 v_{s,2}}$$

and the (α, n) reaction rate with the equation

$$\alpha = \frac{S}{MFv_{s,1}} - 1.$$

An assumption is made that the detector efficiency can be measured and/or calculated based on calibrations with known fission sources (i.e., ^{252}Cf). If this is not true, as may be the case for substantially-altered neutron spectra emitted from large matrices, then if the multiplication can be held at 1, α can be determined and used to solve for F , which can then be used to calculate the neutron detection efficiency. [8] Also, multiplication bias and dead time corrections are being neglected here. [8, 11, 14]

2.3 Motivation for Fast-Neutron Counting

At nuclear facilities, domestically and internationally, most measurement systems used for nuclear materials' control and accountability rely on ^3He detectors. These systems depend on well-established relationships to interpret multiplicity-type measurements for verifying quantities of SNM. Due to resource shortages, alternatives to ^3He systems are urgently needed. Additionally, in the near term, the cost of current ^3He based systems continues to increase as the supply cannot meet the demand. This mission also presents the opportunity to broaden the capabilities of these types of measurement systems to improve current multiplicity techniques and expand the scope to encompass advanced nuclear fuels.

2.3.1 Fast-Neutron Multiplicity Objectives

Within this material protection, accounting, and control technology project, INL and UM are working together to design a fast-neutron multiplicity counter with organic liquid scintillators to quantify fissile material mass. With the fast timing properties of liquid scintillators in conjunction with excellent neutron/photon pulse-shape discrimination (PSD), we are designing a multiplicity system that is less prone to detection/characterization errors for high-activity nuclear materials. Due to the direct measurement of fast neutrons from fission, supplementary quantities related to the fission neutron's energy can be also utilized. Also, an organic-liquid scintillation multiplicity system can make use of photon and joint neutron and photon multiplicities to solve for additional unknowns.

The INL and UM contributors have many years of experience with liquid scintillators to measure SNM. The multi-disciplinary design efforts include: state-of-the art neutron/photon PSD techniques, advances in digital data-acquisition and field programmable-gate-array systems (on-the-fly data processing), automated detector gain matching techniques, and novel data-processing techniques.

2.3.2 Performance Improvements

Fast-neutron counting may have several advantages over the thermal and epithermal neutron counters currently used for nondestructive assay of plutonium-bearing packages. Short die-away times (~ 10 ns) allow assay of higher-order multiplicity with fewer random events, assays of samples with high (α, n) source terms, and assays using active interrogation sources. Inspection times required may be significantly reduced while maintaining acceptable measurement precision, higher-throughput operations may be supported, and the faster detector response times may allow for analysis of materials with substantially-higher emission/count rates.

Employing thermal and/or epithermal neutron detectors for coincidence or multiplicity counting typically requires that the emitted neutrons be moderated prior to reaching a detector's active region. Reducing the average fission neutron energy (~ 2 MeV) to a level at which the

necessary capture reaction has a greater probability of occurrence consequently removes much, if not all, of the emission timing information from consideration. Assuming an “optimal” counting gate width that is on scale with detector die-away ($G = \sim 1.26 \tau$) is utilized, a detection system with $\tau = 50 \mu\text{s}$ would have a gate width of $\sim 63 \mu\text{s}$. [8] Comparing this setting with a theoretical fast neutron-based system ($\tau = 50 \text{ ns}$, $G = 63 \text{ ns}$), the system with a long die-away would be subject to as many as three orders of magnitude more accidentals than would the fast die-away system. Further, a system that operates on timescales comparable with the timescale of fission chain production also allows for the resolution of uncertainties in multiplication and detection efficiency. [15] An additional disadvantage of moderating neutrons prior to their detection is the initial energy information of the detected neutron is lost. With a scintillator-based system, or similar fast neutron-based system, at least some portion of the neutron’s energy information is retained. By combining an energy discrimination capability with the aforementioned short counting gate width, items with elevated (α, n)-to-spontaneous fission ratios can be assayed in reasonable time periods; the potential also exists for improved signal-to-background ratios for active interrogation. [16]

To illustrate the comparison between fast neutron and thermal neutron-based systems a computer code based on the well-known "Ensslin Figure-of-Merit" algorithms was developed to calculate assay uncertainties for various system parameters. [2] Some example results from this code are illustrated in Figure 1, showing (left) the calculated relative standard deviation (RSD) as a function of sample mass for a representative detection system. Calculations of measurement precision for the individual singles, doubles, and triples rates, as well as the total assay precision, were completed for a range of sample masses. The count time was set at 1000 s, $\tau = 50 \mu\text{s}$, $G = 1.257 \cdot \tau$, $P_d = 1.5 \mu\text{s}$, and $\varepsilon = 0.35$. At lower masses the spontaneous emission rate is relatively low; hence, the detection/count rate is also low. As a result, accidental coincidences are minimal and the RSD is dominated by detector efficiency. At higher masses the count rate correspondingly increases, leading to a substantial increase in the number of accidental coincidences. In this case, the RSD is heavily influenced by the detector die-away. In contrast, Figure 1 (right) presents equivalent RSD calculations for a faster die-away system (solid lines) with $\tau = 10 \text{ ns}$, $G = 1.257 \cdot \tau$, and $P_d = 1.5 \text{ ns}$. This plot includes the longer die-away RSD results (broken lines) for comparison. Higher-throughput is much less of an issue due to a significantly reduced number of accidental coincidences over the same measurement time. Quantitatively, for a 20-g ^{240}Pu sample mass, the RSD for the 50- μs die-away time is 2.9%, while the RSD for $\tau = 10 \text{ ns}$ is only 0.3%. For equivalent count times the faster die-away system’s RSD is an order of magnitude less than the slower system. Below 20 g, for these particular sets of detector parameters, the separations between the RSD’s become smaller until they are essentially equal (below $\sim 1 \text{ g}$). In contrast, for masses above 20 g, the separation continues to increase.

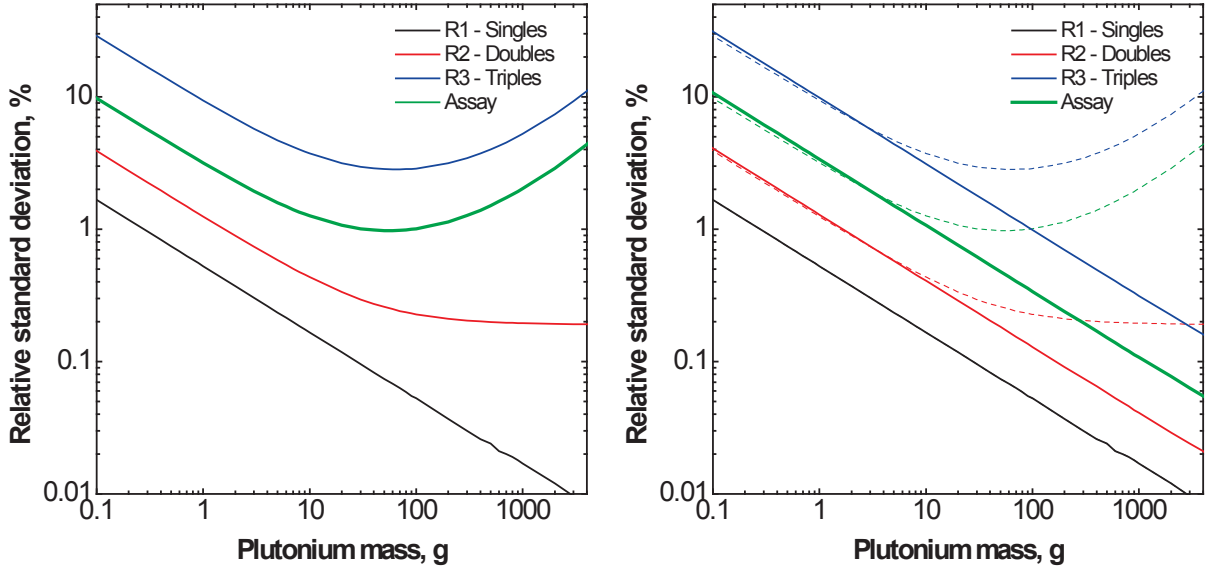


Figure 1. Calculated RSD (%) versus sample mass for representative detection systems. Left: slow die-away system with $\tau = 50 \mu\text{s}$, $G = 1.257\tau$, $P_d = 1.5 \mu\text{s}$, and $\varepsilon = 0.35$. Right: fast die-away system (solid lines) with $\tau = 10 \text{ ns}$, $G = 1.257\tau$, $P_d = 1.5 \text{ ns}$, and $\varepsilon = 0.35$. Calculations for the longer die-away system (broken lines) are included for comparisons.

Aside from neutron detection efficiency, the die-away time of the detector is perhaps the most critical component of the multiplicity counter. [2] Simply stated, a detection system with a minimal die-away time allows for a correspondingly short counting gate width, and thus, fewer accidental coincidences. RSD's for several sample cases as a function of detector die-away time are shown in Figure 2. For $\tau = 70 \mu\text{s}$, increasing the sample mass from 20 g ($M = 1$) to 200 g ($M = 1.2$), while maintaining $\alpha = 1$, only degrades the assay precision by a factor of ~ 2 . However, with the same sample mass of 20 g, increasing α to 10 results in an RSD ~ 23 times larger than the $\alpha = 1$ case. Similarly, the RSD for the 200 g, $\alpha = 1$ case is ~ 23 times smaller than the 200 g, $\alpha = 10$ case. Clearly, increasing the (α, n) rate significantly degrades the assay RSD.

Despite the strong decrease in assay RSD with decreasing detector die-away, a sharp increase in the RSD for τ values below a few μs is seen in the right panel of Figure 2. This trend is an artifact of maintaining a constant predelay with varying detector die-away. With a typical shift register circuit, a predelay is employed to minimize artificial counting due to noise and pileup in the detector electronics. Mathematically, P_d influences the assay RSD within the fraction of signal-triggered events, E_k , detected during the counting gate width ($E_k \propto (e^{-P_d/\tau})^k$). [8] Hence, if P_d is small relative to τ , the sharp rise seen in the right panel of Figure 2 is not nearly as significant. For the data shown in the plot to the right, $P_d = 1.5 \mu\text{s}$. In contrast, the left panel of Figure 2 shows the corresponding assay RSD for a fast neutron detector as a function of die-away time (0 to 100 ns), but with the predelay set to 1.5 ns. Finally, comparing the data from both plots in Figure 2, for a 20 g sample ($M=1$, $\alpha=1$), using the fast neutron counter parameters improves the RSD by a factor of ~ 10 for the same counting period (1000 s). Or, if the same RSD is maintained, the required count time for the fast neutron system would decrease by a factor of ~ 10 .

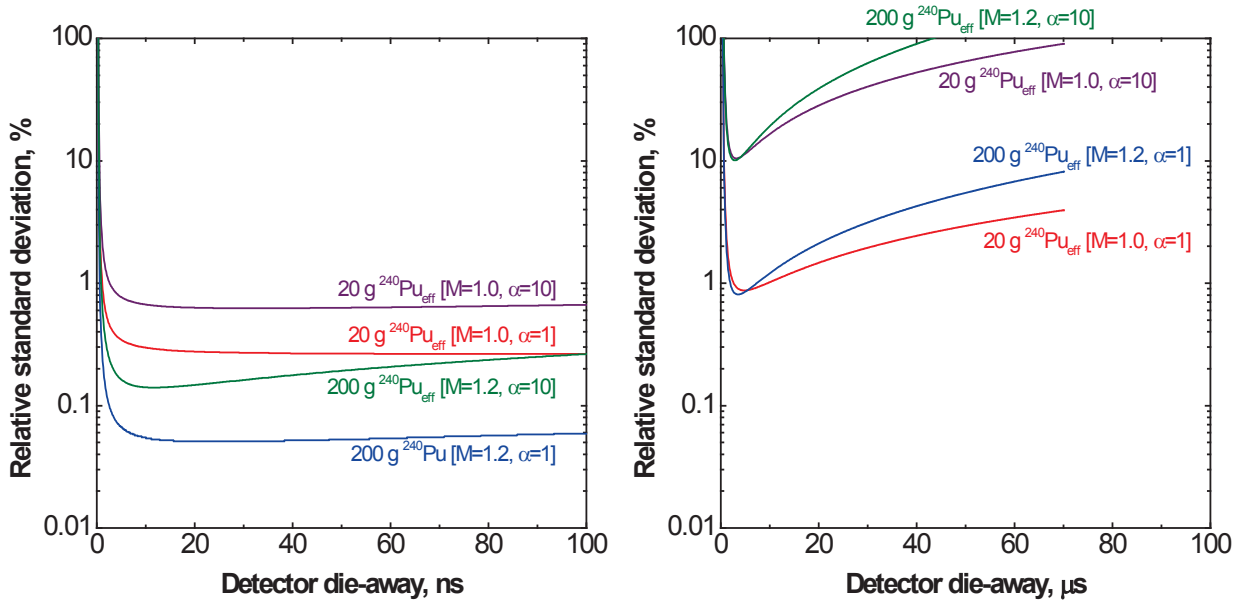


Figure 2. Calculated RSD (%) versus detector die-away times for representative detection systems. Left: short predelay with $G = 1.257\tau$, $Pd = 1.5$ ns, and $\varepsilon = 0.35$. Right: typical thermal neutron detection system predelay with $G = 1.257\tau$, $Pd = 1.5$ μ s, and $\varepsilon = 0.35$.

3 UNIVERSITY EFFORTS

The principle outcome from the University of Michigan team was the successful doctoral dissertation defense by Jennifer L. Dolan in May. [17] Dr. Dolan has been a critical element of this project from its onset.

Another notable outcome from the University of Michigan is the development of simplified assay methods for low ^{240}Pu mass scenarios. These methods take advantage of the negligible accidental coincidence detection rates achieved with fast detectors along with fact that double coincidence uncertainties converge at a much higher rate than that of triple coincidences. A calibrated conversion can be made by fitting the double coincidence detection rate as a function of effective ^{240}Pu mass. Examples of two calibration fits are shown below in Figure 3. While the simplified method is highly dependent upon detectors and their calibration, it can provide a quick and accurate assessment of smaller masses that does not require triple coincidence uncertainty convergence.

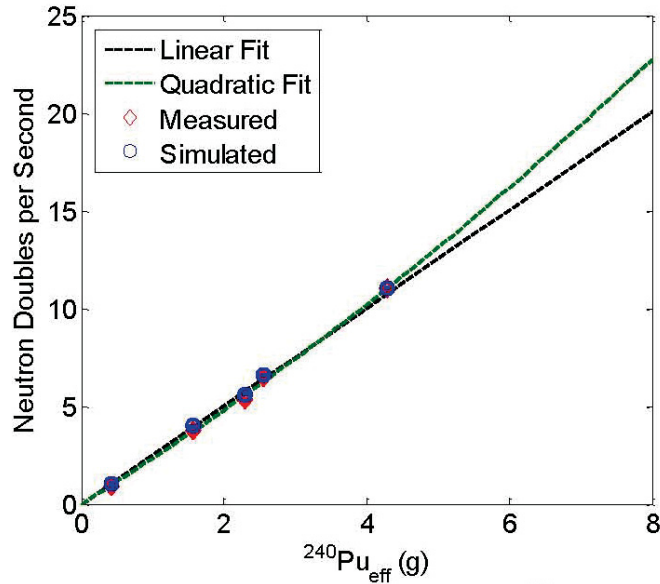


Figure 3. Linear and quadratic fits to PuO₂ double coincidence detection rates versus effective ²⁴⁰Pu mass.

A full dissemination of the work performed at the University of Michigan in FY2013 is provided in Dr. Dolan's dissertation. [17]

4 FAST NEUTRON MULTIPLICITY COUNTER PROTOTYPE DESIGN

The principal objective of this project was the development of a fast neutron multiplicity counter based on liquid scintillation detectors to replace and build upon existing counter technologies. Several design goals were put in place during the development process. First, the multiplicity counting system must have neutron detection efficiency high enough to detect both double and triple coincidences. Second, electronic dead-time losses must be minimized to allow for full advantage to be taken of the fast die-away properties of the liquid scintillators. The system must also be to quantify and extensive range of plutonium masses with highly varied material compositions. Finally, the system geometry must be insensitive to how the sample is positioned inside the counter.

During the latter half of FY2013 a final system design was conceived in preparation of construction of a prototype fast neutron multiplicity counter. Previous efforts on this project guided the final configuration. [17] The design was based on commercially available liquid scintillators that have a 7.62 cm by 7.62 cm by 7.62 cm cubic volume of standard scintillating material (such as EJ-309). A total of 32 scintillators were arrayed in 4 rings of 8 detectors, positioned in such a way that where possible, the photomultiplier tubes for each detector extend vertically between adjacent detectors in an upper or lower ring. This arrangement minimizes the footprint of the system, limiting it to a cylindrical volume with a diameter of approximately 45.25 cm and a height of approximately 57.6 cm assuming a total photomultiplier tube length of 19.8 cm. The sample cavity was designed to be identical in size to that of the JCC-31 High Level Neutron Coincidence Counter (HLNCC) sold by CANBERRA. The cavity had a cylindrical volume with a diameter of 17 cm and a height of 41 cm. The sample cavity was

shielded with lead to attenuate gamma background levels. For all calculations described in this report the lead shielding had a thickness of 0.5 cm, but this can be increased up to a thickness of 6.5 cm if the application demands. Data acquisition electronics include a pair of Struck Innovative Systeme model 3316 digitizers controlled by in-house developed software.

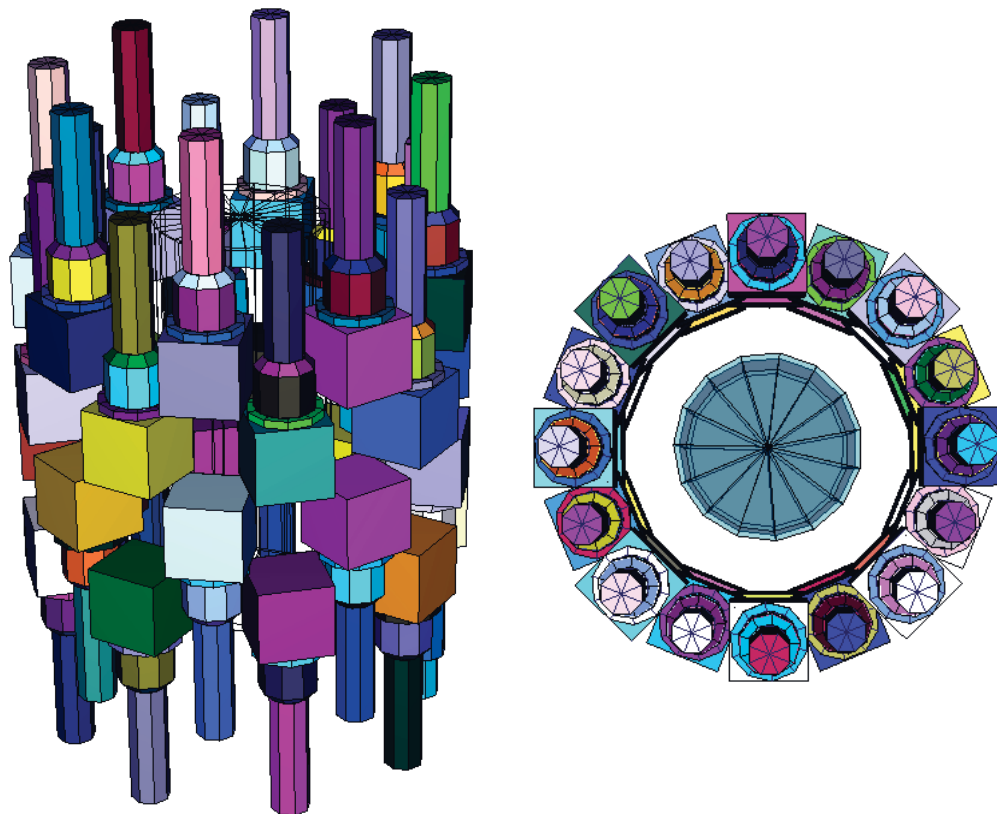


Figure 4. Side and top-down views of the FNMC prototype design from an MCNPX model.

The system was modeled using MCNPX version 2.7.0 and MCNPX-PoliMi version 2.7 to calculate several detection characteristics that included absolute neutron efficiency and the intrinsic die-away constant. [18, 19, 20] A schematic of this modeled geometry is shown in Figure 4. The Monte Carlo models focused on simulating measurements of a ^{252}Cf spontaneous fission source that is built into the MCNPX-PoliMi code. A post-processor analysis code was written that expands upon the MPPost software distributed with MCNPX-PoliMi. [21] MPPost converts neutron scattering events occurring in the detector volume (inventoried in a MCNPX-PoliMi output file) and converts them into light pulses based on the parameters of the detection system. The enhanced post-processor takes the methodology a step further, allowing for the elimination of nearest-neighbor coincidences that occur from cross-talk in the detectors.

Table 1 summarizes the efficiency calculations for the FNMC prototype. These values are presented for neutron energies equivalent to that of a ^{252}Cf spontaneous fission emission spectrum. It may be necessary to increase the pulse height detection threshold beyond the nominal 70 keVee value generally used for fast neutron measurements in order to achieve adequate pulse shape discrimination when assaying samples with very high photon emission

rates. Hence, efficiency values were calculated for threshold levels of 70 keVee, 500 keVee, and 1.0 MeVee. A time-dependent neutron detection spectrum was calculated using the same source and subsequently fit with an exponential curve. The fit resulted in an intrinsic neutron die-away constant of approximately 5.9 ns.

Table 1. Calculated absolute threshold values for the FNMC prototype for several pulse height detection thresholds.

Pulse Height Threshold (keVee)	Calculated Absolute Efficiency
70	9.3%
500	1.6%
1000	0.4%

A Rossi-Alpha distribution was generated from the simulation of a 60-s long measurement of a 1.0- μ Ci ^{252}Cf source, demonstrating the temporal dissemination of coincident counts that originate simultaneously by the system. The distribution is plotted in Figure 5 with and without the application of nearest-neighbor rejection. The rejection method reduces counts in the 30-ns wide ‘reals plus accidentals’ window (green) and ‘accidentals’ window (orange) by approximately 28% and 20% respectively. This figure also clearly demonstrates one of the major benefits of using fast detectors that allow for short (tens of ns) coincidence gates: the ratio of counts of the two counting windows is 0.25% and 0.29% for with and without nearest neighbor rejection respectively. The short counting windows drive accidental coincident count rates down to near negligible levels.

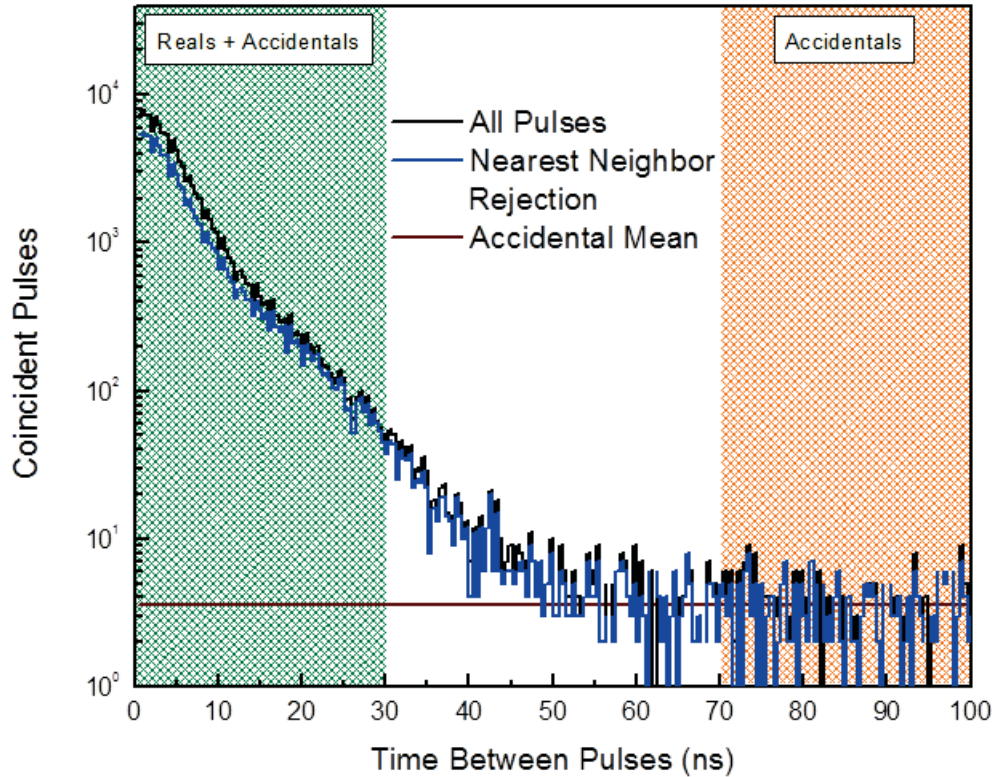


Figure 5. Rossi-Alpha distribution generated from the simulation of a 60 second long measurement of a 1.0 μCi ^{252}Cf source. The application of nearest-neighbor rejection methods is shown in blue.

4.1 Prototype Performance Comparison

An analytical comparison of the prototype fast neutron multiplicity counter and CANBERRA's JCC-31 HLNCC using the assay variance calculation methods described above in Section 2.3.2. [1, 2] HLNCC system parameters were either taken directly from the stat sheet on the CANBERRA website or from a similar study performed at Los Alamos National Laboratory. [2] System parameters for the FNMC prototype that could not be determined from simulations were assumed. Table 2 summarizes the parameters used in the calculations for both of the detection systems.

Table 2. System parameter values used for the analytical performance comparison of the prototype fast neutron multiplicity counter and CANBERRA’s JCC-31 High Level Neutron Coincidence Counter.

System Parameter	FNMC	JCC-31 HLNCC
Absolute Neutron Efficiency	9.3%	17.8%
Die-Away	5.9 ns	42 μ s
Coincidence Gate Width	30 ns	64 μ s
Gate Pre Delay	0 ns	4.5 μ s
Absolute Gamma Efficiency	0.0%	0.0%

It should be noted that these calculations are estimations of the assay variance, and in practice have been shown to be an over prediction of uncertainty by upwards of 50%. [2] The calculations do serve as a useful figure-of-merit for system optimization and optimizations. Background rates other than emissions from (α ,n) reactions and within the sample and system dead times were neglected for this comparison.

Figure 6 is a comparison of the calculated assay variances as a function of time for the prototype FNMC and the JCC-31 HLNCC. Values for the FNMC are shown with solid lines, while the HLNCC values are shown with dashed lines. The top plot has values for 100 g of ^{240}Pu , while the bottom has those for 1 kg. This figure clearly demonstrates how a fast detector system has the ability to confirm mass assay values with much shorter measurement times than the moderated thermal capture-based system. After a 2.5 hour long assay, the prototype FNMC results have a calculated variance percentage approximately 2 orders of magnitude lower than that of the HLNCC. This figure also shows how the influence of (α ,n) reaction rate on mass variance is diminished with the faster system. Again, faster die-away allows for shorter coincidence windows, reducing the probability for false coincident neutron contributions.

Error! Reference source not found. is a plot of the prototype FNMC (upper plot) and the HLNCC (lower plot) mass assay variance as a function of ^{240}Pu mass in the assay sample. Data is shown for 1, 5, and 10 minute assay times. The overall trend for the prototype system is that uncertainty continues to decrease exponentially with increasing ^{240}Pu mass before hitting a mass threshold where the benefits of elevated fission rates become outweighed by detector dead times from high trigger rates and background contributions from alpha-induced neutron production rates. For the high-alpha scenario in these plots (dashed lines) the mass threshold occurs around 1 kg of ^{240}Pu for the FNMC and nearly 1000 times lower for the HLNCC. This figure clearly demonstrates the need for extended assay times for thermal neutron detection based systems to achieve performance levels comparable to fast system for mid to high level mass assays.

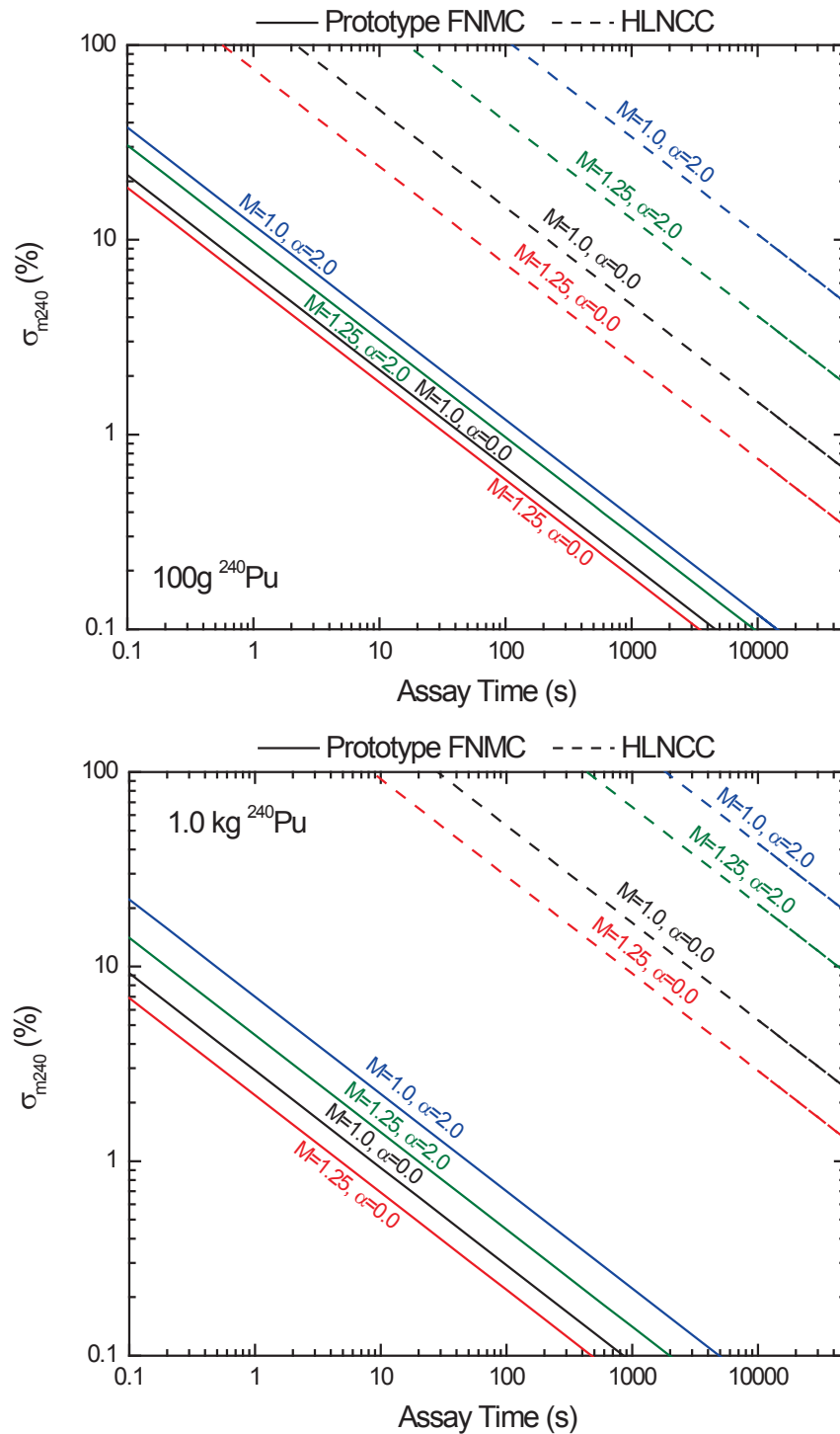


Figure 6. Percent mass variance as a function of assay time for several different measurement scenarios. Values for the FNMC are represented with solid lines, while those for the JCC-31 are shown with dashed lines. Values are given for ^{240}Pu masses of 100 g (top) and 1 kg (bottom).

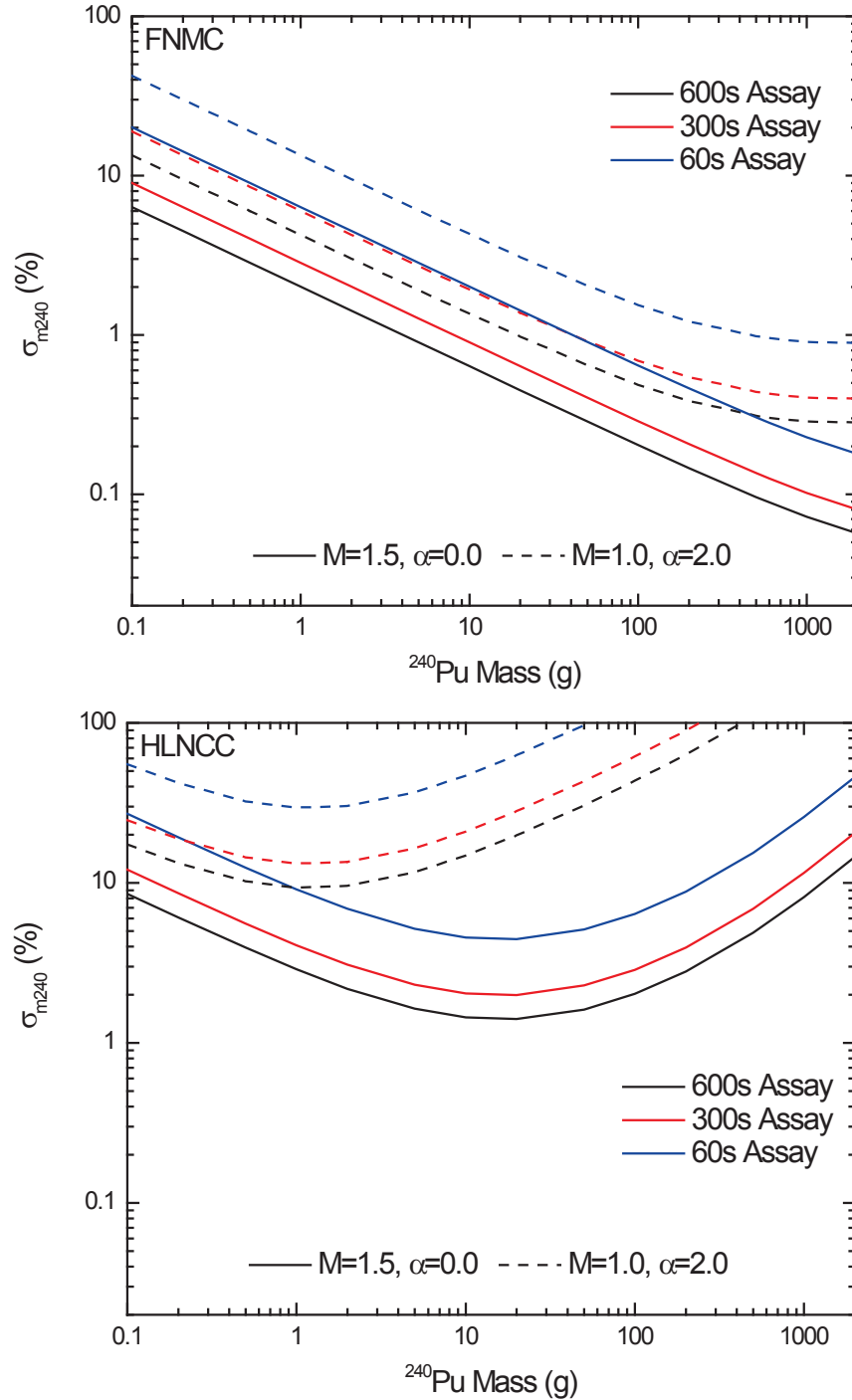


Figure 7. Assay variance for the prototype FNMC (top) and the HLNCC (bottom) as a function of ^{240}Pu mass. Values are provided for 60-s (blue), 300-s (red) and 600-s (black) measurement periods. High-multiplication low-alpha and low-multiplication high-alpha rate scenarios are shown by solid and dashed lines respectively.

4.2 Analytical Parameter Study

A parameter study of proposed system was performed using analytical methods described in the previous section. The prototype's performance was calculated using the estimated mass variance as a figure-of-merit. A software widget was developed for this study to aid in the automation of the calculations, allowing for parameters to be changed quickly and reliably with little effort. The system prototype parameters investigated included absolute neutron detection efficiency, coincidence gate width, and neutron detection die-away constant. The authors have reservations with how neutron and gamma background values are accounted in these analytical methods. Hence, all background rates were assumed to be zero and system pulse shape discrimination methods were assumed to be 100% efficient. Two assay scenarios are considered for every calculation in an effort to bound the problem. These include an 'easy' scenario with a high leakage multiplication without alpha induced neutron contributions and a more difficult scenario with no measurable leakage multiplication and a high alpha reaction rate.

Figure 8 shows the effects of absolute neutron detection efficiency upon the estimated mass assay variance. Ten minute assay times were used for all shown values. The mass uncertainty drops dramatically in all calculated scenarios up to approximately 10% efficiency. Between 10 and 30 percent the benefit of increased efficiency is less than a 50% decrease in variance for all instances shown. The upper-end efficiency value of 30% on this figure is a close approximation of 100% solid angle coverage using the liquid scintillator detector components of the prototype design. System performance could be increased by the inclusion of additional detector rings to the design; however the resulting improvement to solid angle coverage would not be substantial. Linear increases in the cost of hardware, electronics, and system size and weight would not have corresponding increases in detection efficiency, let alone performance. We believe the 9.3% absolute neutron efficiency achieved by the 32 detector, 4 ring design of prototype design (denoted by the vertical green line in the figure) to be very close to an optimal configuration.

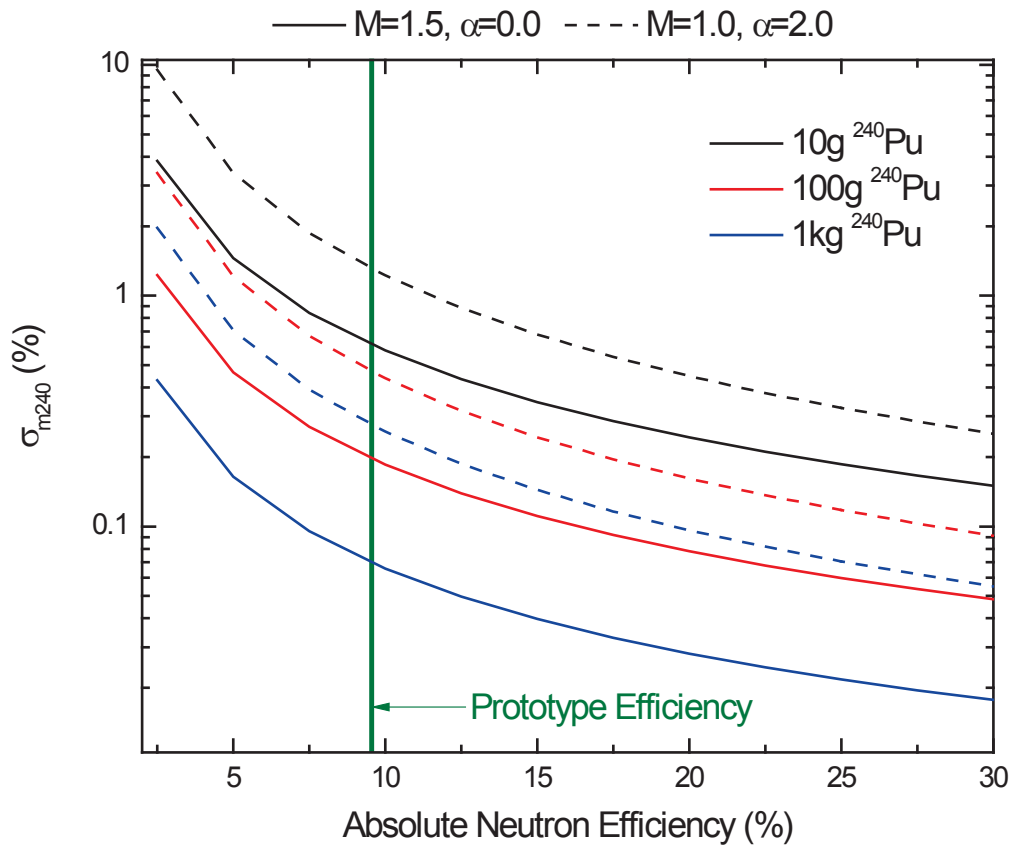


Figure 8. Assay variance for the prototype FNMC as a function of neutron detection efficiency. Values are provided for 60-s (blue), 300-s (red) and 600-s (black) measurement periods. High-multiplication low-alpha and low-multiplication high-alpha rate scenarios are shown by solid and dashed lines respectively.

The effects of coincident window width on estimated assay variance are shown in Figure 9. Ten minute assay times were used to calculate these values. It is clear in this figure how the benefits of increased gate width stop between 10 and 15 ns. For larger masses the uncertainty actually begins to increase with longer window size. Although the performance gain would be small according to these calculations, it may be beneficial for the prototype coincidence window width to be cut in approximately half. This system parameter can be adjusted in software but may be limited by hardware sampling resolution.

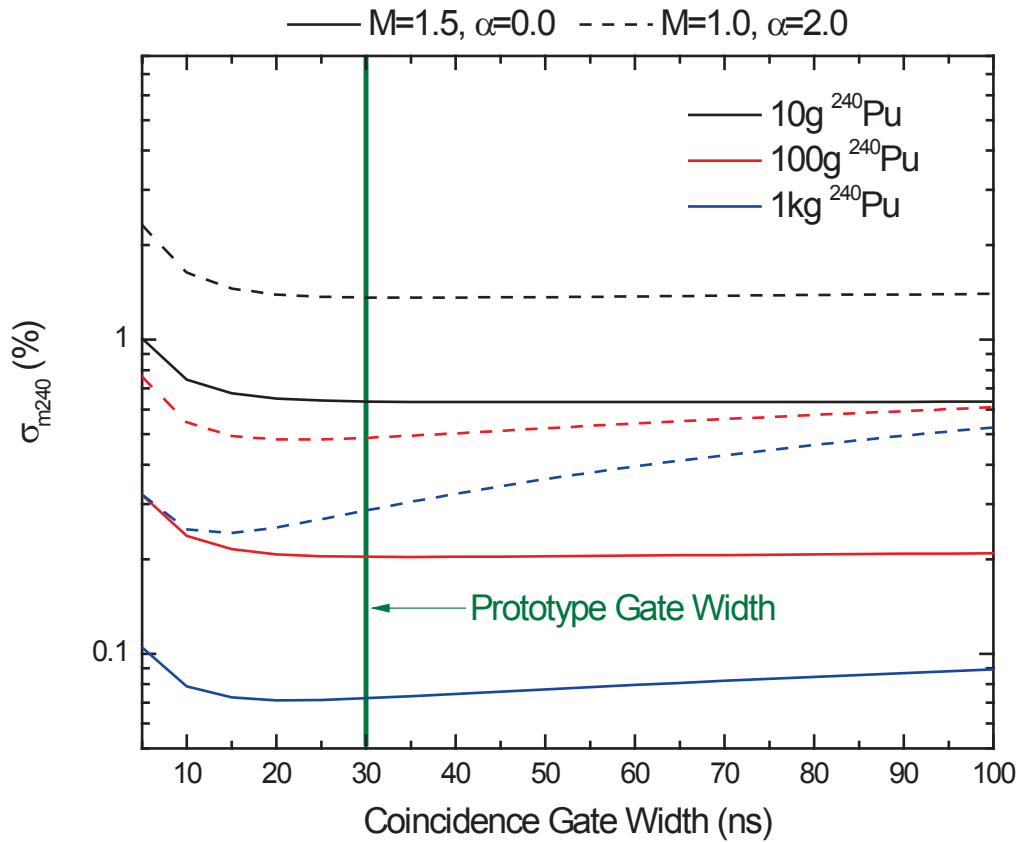


Figure 9. Assay variance for the prototype FNMC as a function of coincidence window width. Values are provided for 60-s (blue), 300-s (red) and 600-s (black) measurement periods. High-multiplication low-alpha and low-multiplication high-alpha rate scenarios are shown by solid and dashed lines respectively.

Figure 10 shows the effects of changing neutron die-away constant on the assay variance. As in the previous 2 figures, the values were calculated using a 10 min measurement time. The benefits of a multiplicity counter with fast neutron die-away have been repeated throughout this report. For the chosen operating parameters of the prototype system, the elevation in performance from decreased die-away constant stops around a value of 8-10 ns. The intrinsic value of the system (approximately 6 ns, shown by the vertical green line in the figure) is not something that can be adjusted without changing the geometry of the scintillating volumes. However, this figure demonstrates how the corresponding drop in performance is trivial for problems bounded by this parameter study and may be significantly outweighed by the decrease in pulse shape discrimination efficiency caused by the increase detector volume.

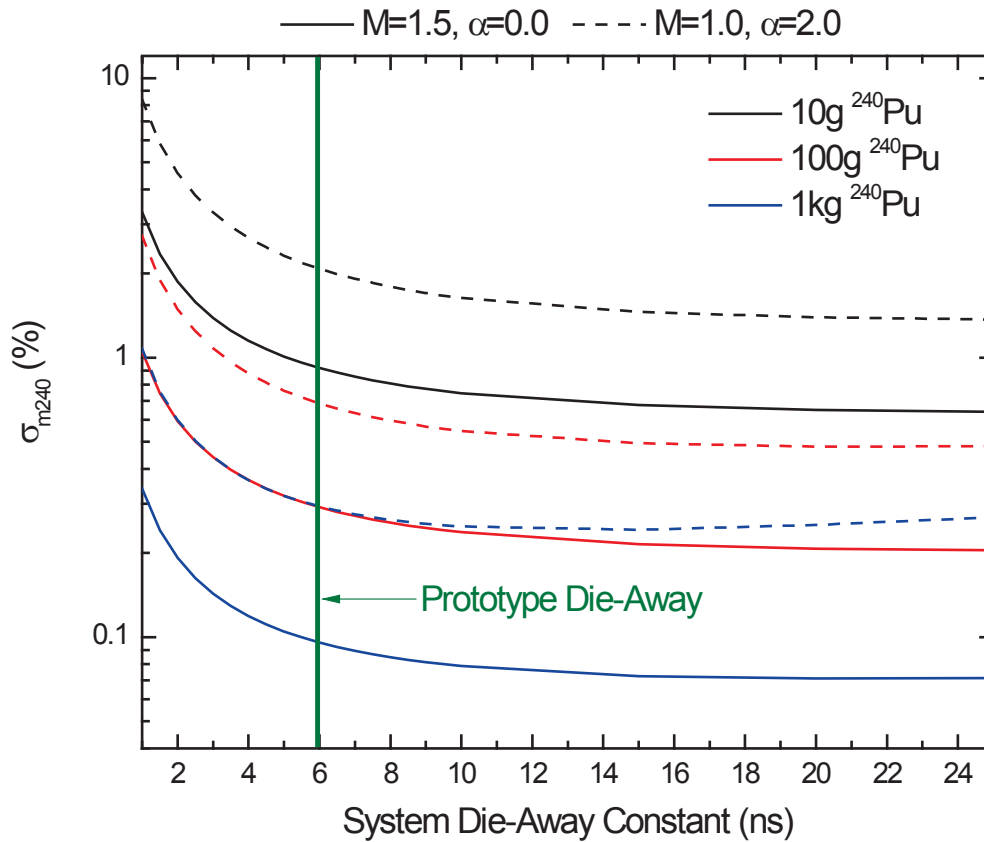


Figure 10. Assay variance for the prototype FNMC as a function of detection system die-away. Values are provided for 60-s (blue), 300-s (red) and 600-s (black) measurement periods. High-multiplication low-alpha and low-multiplication high-alpha rate scenarios are shown by solid and dashed lines respectively.

4.3 Current Prototype Status

INL has received the first of two Stuck model SIS3316 analogue-to-digital converters (ADC) for use in the FNMC prototype. A picture of this state-of-the-art digitizer board is shown in Figure 11. The SIS3316 has the ability to sample at a rate of 250 million samples per second with 14-bit resolution, simultaneously on each of its 16 channels. The key feature of the Struck card that make it favorable over other ADCs is its onboard field-programmable gate arrays (FPGA) that allow for on-the-fly pulse shape discrimination. This feature allows for optimized data handling for minimized electronics dead time.



Figure 11. Photograph of the Struck model SIS3316 digitizer.

Extensive initial testing has been performed with the SIS3316 in anticipation of the FNMC prototype construction. The tests have utilized available 15.0-cm × 15.0-cm × 8.2-cm EJ-309 liquid scintillators and a time-tagged ^{252}Cf spontaneous fission neutron source. A sample setup from the testing is shown in Figure 12. The focus of these measurements was to increase familiarization with the new technology and to begin development of software to control the hardware. The envisioned controlling software package will include algorithms for automated gain matching of the prototype's detector array as well as built in data analysis processes for mass assay determination.

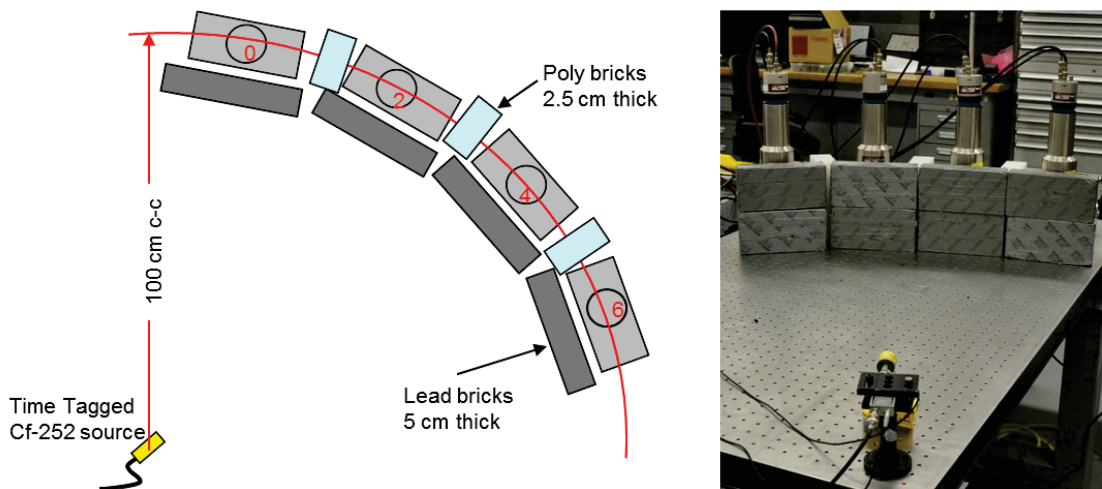


Figure 12. A sample setup from the initial testing of the Struck SIS3316 digitizer.

Several of the SIS3316 tests have focused on optimizing the pulse shape discrimination methods of the onboard field programmable gate arrays. Using the time tagged ^{252}Cf source allows for time-of-flight neutron spectroscopy in tandem with the standard pulse shape discrimination techniques. This combination of analysis methods provides an accurate estimation of the efficiency of the pulse shape discrimination methods. Figure 13 demonstrates how this technique works. This data were collected with a single liquid scintillator described above positioned 110 cm from the ^{252}Cf source. The time-of-flight spectra show a clear neutron flight time below which it would be impossible to detect fission energy neutron emissions originating from the ^{252}Cf source. For the data shown in Figure 13 this occurs at approximately 35 ns. The SIS3306 digitizes the pulse waveforms by analyzing pulse heights in several adjustable windows surrounding and including the actual pulse. A pulse shape value is produced by taking ratios of desired windows and their sums. The plot in this figure is color coded by

pulses with pulse shape values grouped according to the key in the upper corner. For example, a pulse shape threshold value of 1.0 reduces photon contributions by 98.9% while discriminating 15.4% of the counts in the neutron region of this data set.

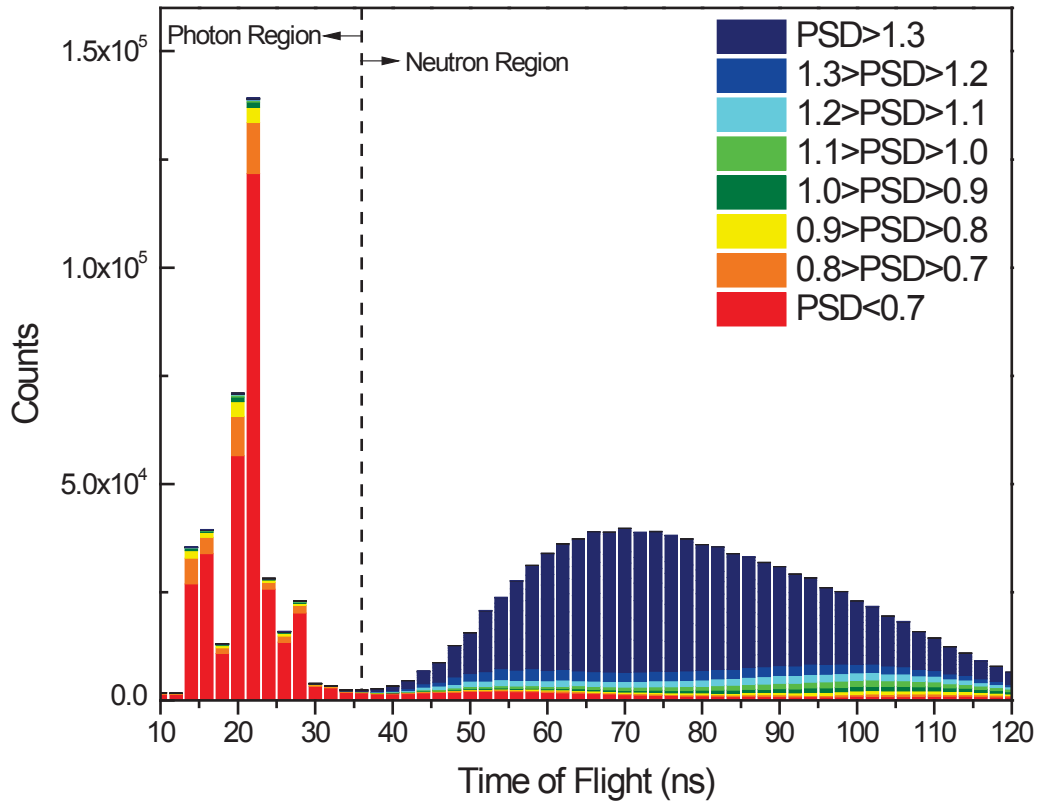


Figure 13. An example of a neutron time-of-flight measurement using the Struck SIS3316 pulse shape discrimination methods. A single liquid scintillator placed 110 cm from the time tagged ^{252}Cf source was used to collect the data. Colored regions represent similar pulse shape analysis values for use in neutron/photon discrimination. Pulses with pulse heights below 650 keVee were discarded from this data set.

Currently further production efforts on construction of the fast neutron multiplicity counter have been put on hold until authorization is received to purchase the required hardware. A high-level of proficiency has been reached with the currently-procured components. Prototype construction is required for further optimization.

5 SUMMARY

The FY2013 efforts for this project resulted in the design of a prototype fast neutron multiplicity counter leveraged upon the findings of previous project efforts. The prototype design includes 32 liquid scintillator detectors with cubic volumes 7.62 cm in dimension configured into 4 stacked rings of 8 detectors. Detector signal collection for the system is handled with a pair of Struck Innovative Systeme 16-channel digitizers controlled by in-house developed software with concomitant multiplicity analysis algorithms. Initial testing and familiarization of the currently obtained prototype components is underway, however full prototype construction is required for further optimization.

Monte Carlo models of the prototype system were performed to estimate die-away and efficiency values. Analysis of these models resulted in the development of a software package capable of determining the effects of nearest-neighbor rejection methods for elimination of detector cross talk. A parameter study was performed using previously developed analytical methods for the estimation of assay mass variance for use as a figure-of-merit for system performance. [1, 2] A software package was developed to automate these calculations and ensure accuracy. The results of the parameter study show that the prototype fast neutron multiplicity counter design is very nearly optimized under the restraints of the parameter space.

Also of note, Jennifer L. Dolan, a graduate student that has been a part of the project from its onset, successfully defended her doctoral dissertation in May of 2013.

6 REFERENCES

- [1] I. Pazsit, A. Enqvist and L. Pal, "A Note on the Multiplicity Expression in Nuclear Safeguards," *Nucl. Inst. Meth. Phys. Res. A*, vol. 603, pp. 541-544, 2009.
- [2] N. Ensslin, N. Dytlewski and M. S. Krick, "Assay Variance as a Figure of Merit for Neutron Multiplicity Counters," *Nucl. Inst. Meth. Phys. Res. A*, vol. 290, pp. 197-207, 1990.
- [3] D. L. Chichester and et al., "FY09 Advanced Instrumentation and Active Interrogation Research for Safeguards," Idaho National Laboratory, Idaho Falls, ID, 2009.
- [4] D. L. Chichester and et al., "MPACT FY2011 Advanced Time Correlated Measurement Research at INL," Idaho National Laboratory, Idaho Falls, ID, 2011.
- [5] D. L. Chichester and et al., "MPACT Fast Neutron Multiplicity System Design Concepts," Idaho National Laboratory, Idaho Falls, ID, 2012.
- [6] "Ne.doe.gov," [Online]. Available: <http://www.ne.doe.gov/AFCI/neAFCI.html>. [Accessed Aug 2012].
- [7] "Un.org," 1968. [Online]. Available: <http://www.un.org/disarmament/WMD/Nuclear/NPT.shtml>. [Accessed Aug 2012].
- [8] N. Ensslin and et al., "Application Guide to Neutron Multiplicity Counting," Los Alamos National Laboratory, Los Alamos, NM, 1998.
- [9] "CANBERRA Industries," [Online]. Available: <http://www.canberra.com/>.
- [10] "Canberra.com," 2000. [Online]. Available: http://www.canberra.com/products/waste_safeguard_systems/neutron-safeguards-systems.asp. [Accessed Sept 2012].
- [11] D. Reilly, N. Ensslin, H. Smith and (eds.), "Passive Nondestructive Assay of Nuclear Materials," U. S. Nuclear Regulatory Commission, Washinton, D. C., 1991 and 20074.

- [12] N. Dytlewski, M. S. Krick and N. Ensslin, "Measurement Variances in Thermal Neutron Coincidence Counters," *Nucl. Inst. Meth. Phys. Res. A*, vol. 327, pp. 469-479, 1993.
- [13] J. M. Verbeke, C. Hagmann and D. Wright, "Simulation of Neutron and Gamma Ray Emission from Fission and Photofission," Lawrence Livermore National Laboratory, Livermore, CA, 2010.
- [14] D. Henzlova, "Epithermal Neutron Multiplicity Counter (ENMC) Measurement Description and Results," Los Alamos National Laboratory, Los Alamos, NM, 2010.
- [15] S. McConchie, P. Hausladen and J. Mihalczko, "Prompt Neutron Decay Constant from Feynman Variance Fitting," Oak Ridge National Laboratory, Oak Ridge, TN, 2010.
- [16] M. C. Miller and et al., "Design of a Fast Neutron Coincidence Counter," *App. Rad. Iso.*, vol. 48, pp. 1549-1555, 1997.
- [17] J. L. Dolan, "Safeguarding Special Nuclear Material by Detecting Fast Neutrons in Liquid Scintillators," University of Michigan, Ann Arbor, MI, 2013.
- [18] E. Padovani and et al., "Introduction to MCNPX-PoliMi," University of Michigan, Ann Arbor, MI, 2012.
- [19] D. Pelowitz, MCNPX USER'S MANUAL Version 2.7.0, Vols. LA-CP-11-00438, Los Alamos National Laboratory, 2011.
- [20] S. A. Pozzi, "MCNPX-PoliMi for Nuclear Nonproliferation Applications," *Nucl. Inst. Meth. Phys. Res. A*, vol. 694, pp. 119-125, 2012.
- [21] E. C. Miller and et al., "MCNPX-PoliMi Post-Processor (MPPost) Manual," University of Michigan, Ann Arbor, MI, 2012.